FSS-Enhanced Quasi-Optical Dielectric Measurement Method for Liquid Crystals in Sub-THz Band

Byeongju Moon, *Student Member, IEEE*, and Jungsuek Oh, *Member, IEEE*

***Abstract*—In this letter, the dielectric characterization of nematic liquid crystals (LCs) materials using a complementary split-ring resonator (CSRR) frequency selective surface (FSS) at sub-THz is proposed. The CSRR FSS consists of two printed CSRRs separated by 130 μm thick layer of LCs. Because the metal pattern of the CSRR FSS covers most of the LC area, the director of the LC is well rearranged when an external electric field is applied. High-gain narrow beamwidth ultrathin transmitarrays (TAs) are used to foster a quasi-optical measurement setup instead of a dielectric lens, which is used for a conventional setup. Using TA endows the system with flexibility, such as in the size of the system, by changing the gain of the TA. To extract the dielectric constant and loss tangent of the LCs, it is necessary to shift the resonant frequency and vary the transmission loss. To obtain these data, a CSRR FSS with LCs was placed between two TAs. Finally, by comparing the measured and simulation results, the complex dielectric constants of the LCs were determined using the curve-fitting method.**

***Index Terms*—Complementary split-ring resonators (CSRRs), complex dielectric constant, complex permittivity measurement, free-space measurement, frequency selective surface (FSS), liquid crystals (LCs), quasi-optical, transmitarray (TA).**

I. Introduction

WHILE detailed standards for 6G have not been established, there is considerable attention on the sub-THz frequency bands, which operates above 100 GHz. The high frequencies in the sub-THz band result in differences in the permittivity and loss tangent of materials compared to the millimeter wave band. Accurately determining material properties is crucial for the precise design and analysis of microwave and THz devices, as the complex dielectric constant plays a critical role in device performance. Liquid crystal (LC) materials have recently garnered significant attention, particularly over 100 GHz or higher [1], [2]. LCs offer efficiency, cost-effective features, and ease of manufacture compared to other devices. Most importantly, LCs possess the ability to modify their permittivity in response to an external electric field. This tunability makes LCs highly valuable for advanced communication systems and the design of devices operating in the sub-THz frequency band.

The complex dielectric constant of LCs has been determined using resonant and broadband transmission line methods [3], [4], [5], [6]. In [3] and [5], the resonant method, which is sensitive and provides the exact permittivity value of a dielectric material, was used. The measurements were performed using a rectangular or circular resonator with the LCs placed directly under the resonator. The LCs function as a substrate for the resonator, and the resonant frequency varies with changes in the permittivity of the LCs. Although the resonant method is accurate and sensitive, obtaining the exact value of the loss tangent of dielectric materials is difficult. The broadband transmission line method [4], [6] has an advantage over the resonant method because it obtains both permittivity and loss tangents with fairly accurate values over a wide frequency range. The transmission line method utilizes a transmission matrix and *S*-parameters to extract the dielectric constants of the materials. However, as the frequency increases, it becomes difficult to fabricate the devices because they become extremely small.

In this letter, the dielectric characterization of an LC using a complementary split-ring resonator (CSRR) frequency selective surface (FSS) in the sub-THz band is proposed. Although the proposed CSRR FSS is one type of resonant method, not only can the exact value of the permittivity be obtained but the precise value of the loss tangent can also be determined. A high-gain narrow beamwidth ultrathin TA [7] offers a quasi-optical measurement setup similar to the finite element method (FEM) simulation environment. The proposed quasi-optical free-space measurement system using high-gain narrow beamwidth TA is presented in Fig. 1. The rest of this letter is organized as follows. Section II describes the CSRR FSS structure and quasi-optical measurement setup utilizing the TA. Section III presents the measurement setup, and the results obtained using the fabricated CSRR FSS are given in Section IV. Finally, Section V concludes this letter.

II. CSRR FSS Structure and Simulation Results

One of the conventional methods for determining the complex dielectric constant is waveguide measurement. The waveguide measurement technique is one of the resonant methods, which uses the resonant peaks of the transmission or reflection loss [8], [9], [10]. FSSs are placed inside the aperture of waveguides and

Manuscript received 22 June 2023; revised 21 July 2023; accepted 26 August 2023. Date of publication 30 August 2023; date of current version 1 December 2023. This work was supported by the Samsung Research Funding Center of Samsung Electronics under Project SRFC-TE2103. *(Corresponding author: Jungsuek Oh.)*

The authors are with the Institute of New Media and Communication (INMC) and the Department fo Electrical and Computer Engineering, Seoul National University, Seoul 08826, South Korea (e-mail: bjmoon5843@snu.ac.kr; jungsuek@snu.ac.kr).

Digital Object Identifier 10.1109/LAWP.2023.3309990

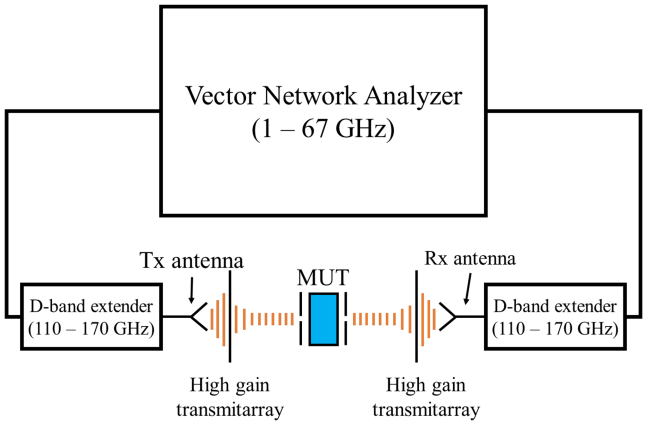

Fig. 1. Illustration of the proposed free-space measurement system with high-gain narrow beamwidth transmitarray (TA) for quasi-optical measurement environment.

a dielectric slab is located between the FSSs. After measuring the resonant peaks, the dielectric constant is determined by calculating equations or using curve-fitting method. The FSS was designed on a low-loss-supporting dielectric substrate to have a mechanically robust setup and maintain deep resonant peaks in the transmission or reflection loss. This method estimates both the real and imaginary parts of the dielectric permittivities of random dielectric materials. However, the problem with this technique is that the FSS must fit the waveguide aperture. For frequency bands above 100 GHz, it is difficult to use the waveguide method, because the aperture dimensions of the waveguide are extremely small. To eliminate this disadvantage and use the principle of the waveguide measurement technique, the large dimension of the FSS is used. The large aperture of the FSS has the same effect as the FSS in the waveguide.

Conventionally, split-ring resonators (SRRs) or CSRRs are used to obtain the dielectric constants of the dielectric materials using the transmission line method [11], [12], [13], [14], [15], [16], [17]. The equivalent circuit model of the CSRR is widely known. Therefore, the resonant frequency was calculated using the capacitance and inductance of the equivalent circuit model. The capacitance of the equivalent circuit changed as the substrate of the CSRR changed. Therefore, the real parts of the complex permittivity and resonant frequency exhibit a linear relationship [18]. The imaginary part of the complex permittivity is extracted using the transmittance or reflectance coefficient amplitude response at the resonant frequency. However, the method mentioned above was applied only up to 5 GHz because manufacturing limitations were reached at a frequency higher than 5 GHz. To overcome this issue, a CSRR FSS [19] was used to measure the dielectric constants in the sub-terahertz frequency bands. As reported in a previous study [20], [21], the CSRR FSS is a high Q bandpass spatial filter and responds to only one polarization incident wave.

The CSRR FSS has another advantage over other FSS structures. As analyzed in [2] and [22], the movement of the director of the LCs depends on the metal patterns on and under the LCs layer. The larger the area occupied by the metal pattern, the wider the range in which the LC molecules align with the external

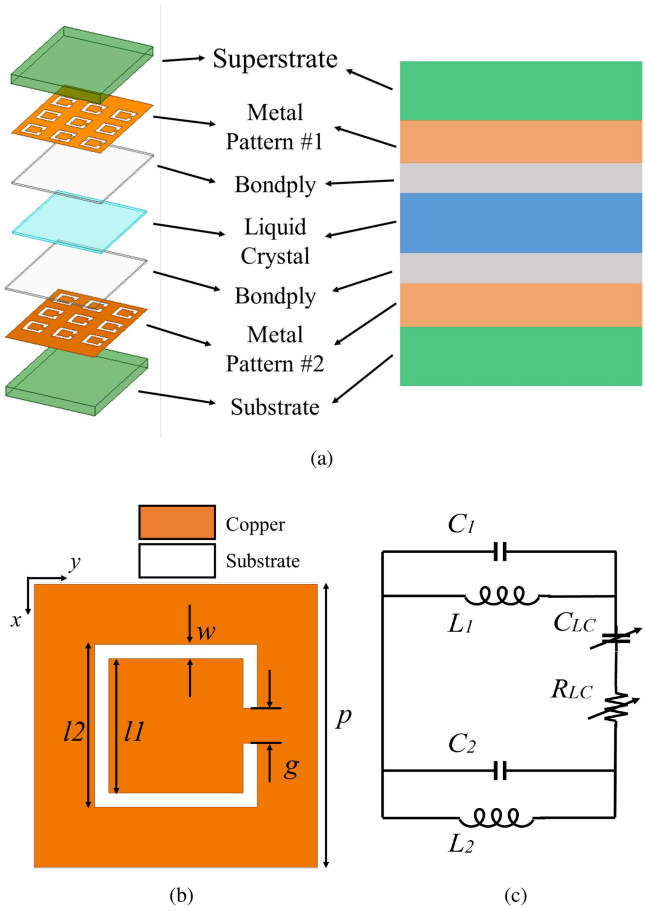

Fig. 2. Proposed LC CSRR FSS. (a) Exploded and side view of the proposed LC CSRR FSS structure. The LC is sandwiched between two substrates and two metal patterns. (b) Top view and parameters of the proposed LC CSRR FSS unit cell. (c) Schematic of the proposed unit cell. As the external electric field is applied, the director of the LCs is rearranged such that C_{LC} and R_{LC} change.

electric field. Most FSS structures are composed of a single metal layer, which is not suitable for applications in external electric fields. In the case of the SRR, the uncovered area with a metal pattern is larger than the covered area. This makes it highly likely that when an external voltage is applied, there is a region where the molecules of the LCs are not properly arranged. In contrast, in the case of CSRR, the metal pattern covers most of the area; therefore, the LC director gets fully aligned with the external electric field.

The proposed LC CSRR FSS is illustrated in Fig. 2, which consists of three planar substrate layers. All three substrates were fabricated by low-cost standard printed circuit board (PCB) manufacturing technology. For the middle layer, LCs are placed to measure the dielectric constant and loss tangent. This LC layer was sandwiched between Taconic TLY-5 substrates with $\varepsilon_{\mathrm{r}} = 2.2$ and $\tan\delta = 0.01$. The thicknesses of the Taconic substrates and LC layer were 0.13 and 0.13 mm, respectively. As mentioned and analyzed in [7], the bondply should be considered because the thickness is thick enough compared to the wavelength. The thickness of the bondply was 40 μm ($\approx$0.02 λ_{o}). The bondply was placed under the copper layer facing the LCs layer. The copper layer, sandwiched between the top and bottom TLY-5

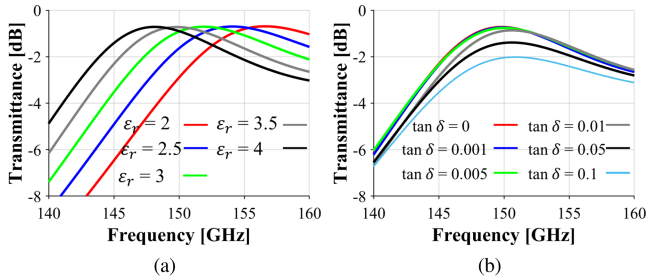

Fig. 3. Simulated results of the proposed LC CSRR FSS. (a) Resonant frequency shifts for TE polarization incident wave according to LC permittivity changes with a fixed loss tangent (tan $\delta = 0$). (b) Transmission loss changes for TE polarization incident wave according to variation of LC loss tangent with fixed permittivity (εr = 3.5).

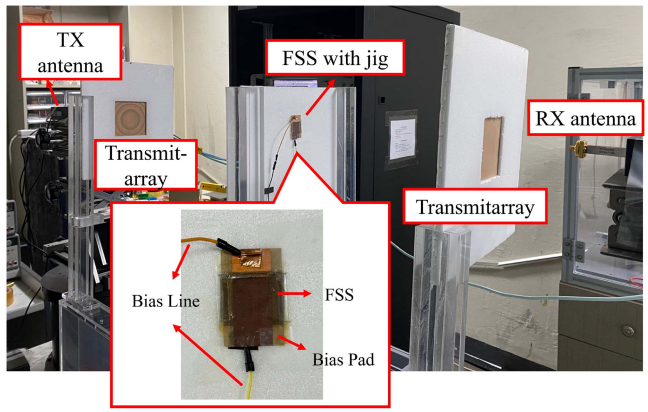

Fig. 4. Measurement setup of the proposed LC CSRR FSS and high-gain narrow beam TA for a quasi-optical environment. To apply the external electric field, the bias lines are attached to the bias pad with copper tape and the bias lines are connected to the dc power supply.

substrates, exhibited an 18 μm thickness. The parameters of the CSRR FSS unit cell are as follows: $p = 0.8$ mm, $l1 = 0.38$ mm, $l2 = 0.45$ mm, and $g = 0.08$ mm. It should be noted that the proposed design can only be applied to TE incident plane waves because of the cross-polarization effect [20]. Therefore, in this letter, only the TE mode incident wave was considered in the simulations and measurements. Fig. 2(c) shows a schematic of the proposed FSS. When an external electric field is applied to the LC, the C_{LC} and R_{LC} change. The variation in capacitance and resistance results in a change in the frequency response of the FSS, as discussed previously.

A Floquet simulation of the proposed unit cell was conducted in the HFSS, and Fig. 3 illustrates the simulated results of the proposed LC CSRR FSS under TE polarization incident wave. As illustrated in Fig. 3(a), the resonant frequency shifts as the permittivity of the LC changes with no loss tangent. When $\varepsilon_{\mathrm{r}} = 2.5$, the resonant frequency was 154 GHz, whereas when $\varepsilon_{\mathrm{r}} = 3.5$, the resonant frequency was 150 GHz. Similarly, the variation in transmission loss as the loss tangent of the LC changes with a fixed permittivity is illustrated in Fig. 3(b). When tan δ was 0.005, the transmission loss was –0.7 dB and when tan δ was 0.01, the transmission loss was –0.9 dB. Dielectric properties of the LC used in the proposed CSRR FSS, GT7-29001 from Merck KGaA, Darmstadt, Germany, are 2.46, 0.0116 ($\varepsilon_{\perp}$) and 3.53, 0.0064 ($\varepsilon_{\parallel}$), respectively, at 19 GHz. Therefore, the proposed CSRR FSS can be used to determine the dielectric constant of the LC in the *D*-band.

III. Quasi-Optical Measurement Environment Setup

For low-frequency bands, to measure the dielectric properties of the material using free-space measurements, the dielectric slab was located on the free-space path between the two horn antennas. However, for the millimeter- and submillimeter-wave frequency bands, antenna beam growth was a major drawback when using a free-space characterization technique to measure the properties of a dielectric slab [23]. This is because the beam tended to spread out as it traveled through free space, resulting in a decrease in the energy concentration on the slab. To overcome this challenge, it is necessary to use special devices such as Gaussian optics lens antennas (GOLAs) to refocus the beam and improve the energy concentration on the slab. This collimated beam of radiation propagation is known as quasi-optical propagation.

Quasi-optical propagation leads to a certain level of certainty in obtaining precise results, reinforcing the robustness and credibility of the acquired data.

In the case of commercially available GOLAs, it exhibited a minimum gain of 25 dBi and a maximum gain of 47 dBi. However, because the fabrication of GOLAs is complicated and expensive, the high-gain narrow beam ultrathin TA [7] is used to achieve quasi-optical propagation on behalf of the GOLA. The major advantage of using an ultrathin TA is the adjustability of the measurement system. The gain and beamwidth of the TA can be easily controlled by deploying a unit cell during fabrication, and it is significantly cheaper than the GOLA. In addition, by changing the gain of the TA, the distance between the sample and the TAs can be determined, indicating that the size of the measurement system can be minimized.

IV. Fabrication and Experimental Results

The proposed LC CSRR FSS was manufactured using a standard PCB process. As mentioned above, two metal layers were printed on the two substrates (Taconic TLY-5). Each substrate layer is glued to a bondply. The length widths of the FSS were 42 and 25 mm. The printed FSS section was 16 mm $\times$ 16 mm, and the cavity for the LC was 20 mm $\times$ 18 mm $\times$ 0.13 mm. The LCs were injected using a syringe through small holes in the substrate.

Fig. 4 shows the measurement setup, which consists of an Anritsu MS4647B vector network analyzer and Tx and Rx VDI WR 6.5 waveguide extenders. As mentioned previously, a high-gain narrow beam [7] was used to create a quasi-optical environment. To minimize the errors during the setup stage, several factors should be considered. First, the positioning and stabilization of the proposed LC CSRR FSS can be achieved by affixing it onto a Styrofoam slab. This placement aims to effectively fix its position and subsequently mitigate potential

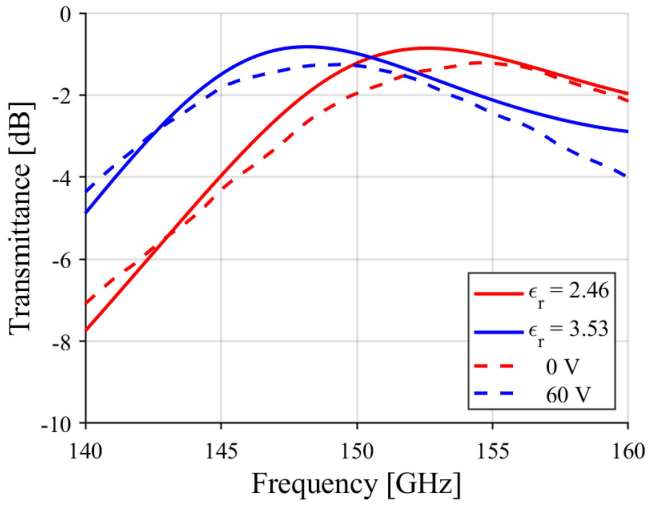

Fig. 5. Measured and simulated spectral transmittance of the LCs-based CSRR FSS. The dotted lines represent the measured results, whereas the solid lines represent the simulated results using the complex dielectric constants value at 19 GHz.

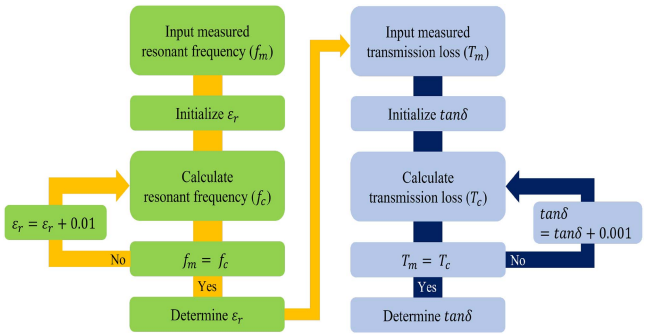

Fig. 6. Process of finding permittivity and loss tangent of the LCs using the measured and calculated values.

measurement errors. A ruler was used to make sure FSS is not tilted while being fixed on the slab. Also, the misplacement of FSS and diffraction and scattering might cause crucial error, so the laser was used to align the TRx, TAs, and the FSS in the straight line. The dc power supply was used to apply an external voltage to the LCs. Additional wires were attached to the extra pad and connected to a dc power supply. The positions of the RF cable and additional wires were fixed to reduce measurement errors.

The experimental and simulated results are plotted in Fig. 5. The dashed lines represent the measured results, whereas the solid lines represent the simulated results using the complex permittivity values at 19 GHz. There is a similar trend between the two results. When the bias voltage was 0 V, the pass band was centered at 154.6 GHz, and when the bias voltage was 60 V, the resonant frequency was shifted downwards to 149.6 GHz, which exhibits a 3.3% tunability. Fig. 6 shows how the complex permittivity values of the LC were determined by curve-fitting process. First, set the dielectric constants of the LCs and determined the resonant frequency of the LC CSRR

TABLE I
COMPARISON OF THE EXPERIMENTAL RESULTS AND OTHER LITERATURES WITH OTHER TYPES OF LCS

Ref	[3]	[4]	[25]	[24]	This work
Range of frequency (GHz)	40	30–60	60	140–165	140–160
LC Type	E7	E7	GT3-23001	GT3-23001	GT7-29001
$\varepsilon_\perp$	2.73	2.78	2.43	2.47	2.43
tan $\delta_\perp$	X	0.0061	0.0131	0.02	0.05
$\varepsilon_\parallel$	3.15	3.25	3.14	3.25	3.57
tan $\delta_\parallel$	X	0.0011	0.0035	0.015	0.037

X stands for "not mentioned."

FSS using an EM simulation. Increment the value by 0.01 until the simulated and measured values agreed. Thereafter, repeat the same procedure on the loss tangent. The complex permittivity value of GT7-29001 was determined, and the values were 2.43 and, 0.05 when not biased and 3.57 and, 0.037 when fully biased. The permittivity values have almost identical values. In Table I, the experimental results and others' values from the works of literature are presented. From [24] the extracted loss tangents of GT3-23001 differ from the values at 19 GHz by a factor of 1.5 and 4.3. The extracted loss tangents of GT7-29001 from measured results differ from the values at 19 GHz by a factor of 4.3 and 5.8. Considering the range and the differences, the extracted complex permittivities are acceptable.

V. CONCLUSION

This letter presents a free-space measurement process for measuring the complex dielectric constants of LCs using a CSRR FSS in sub-THz band. Owing to the characteristics of the CSRR, a high Q frequency response was obtained. Additionally, because the metal pattern covered most of the LCs area, the rearrangement of LCs molecules occurred properly depending on the external dc bias application. The viability of determining the complex dielectric constant of LCs using the proposed CSRR FSS was demonstrated. A quasi-optical measurement environment was developed using a high-gain narrow-beamwidth ultrathin TA. The results are in excellent agreement with those obtained through the numerical analysis. The dielectric constant barely changed, although the loss tangent was considerably different owing to the difference in frequency. Acceptable results were obtained using the proposed method. Therefore, the proposed method can be used to determine the complex dielectric constants of materials in various states, particularly liquid-state materials, which are difficult to measure because of their fluidity.

REFERENCES

[1] W. Hu et al., "Design and measurement of reconfigurable millimeter wave reflectarray cells with nematic liquid crystal," *IEEE Trans. Antennas Propag.*, vol. 56, no. 10, pp. 3112–3117, Oct. 2008.
[2] G. Perez-Palomino et al., "Design and experimental validation of liquid crystal-based reconfigurable reflectarray elements with improved bandwidth in F-band," *IEEE Trans. Antennas Propag.*, vol. 61, no. 4, pp. 1704–1713, Apr. 2013.
[3] M. Yazdanpanahi, S. Bulja, D. Mirshekar-Syahkal, R. James, S. E. Day, and F. A. Fernandez, "Measurement of dielectric constants of nematic liquid crystals at mm-wave frequencies using patch resonator," *IEEE Trans. Instrum. Meas.*, vol. 59, no. 12, pp. 3079–3085, Dec. 2010.

[4] S. Bulja, D. Mirshekar-Syahkal, R. James, S. E. Day, and F. A. Fernández, "Measurement of dielectric properties of nematic liquid crystals at millimeter wavelength," *IEEE Trans. Microw. Theory Techn.*, vol. 58, no. 12, pp. 3493–3501, Dec. 2010.

[5] D. E. Schaub and D. R. Oliver, "A circular patch resonator for the measurement of microwave permittivity of nematic liquid crystal," *IEEE Trans. Microw. Theory Techn.*, vol. 59, no. 7, pp. 1855–1862, Jul. 2011.

[6] P. Deo, D. Mirshekar-Syahkal, L. Seddon, S. E. Day, and F. A. Fernández, "Microstrip device for broadband (15–65 GHz) measurement of dielectric properties of nematic liquid crystals," *IEEE Trans. Microw. Theory Techn.*, vol. 63, no. 4, pp. 1388–1398, Apr. 2015.

[7] D. Seo, H. Kim, S. Oh, J. Kim, and J. Oh, "Ultrathin high-gain D-band transmitarray based on a spatial filter topology utilizing bonding layer effect," *IEEE Antennas Wireless Propag. Lett.*, vol. 21, pp. 1945–1949, 2022.

[8] F. Costa, C. Amabile, A. Monorchio, and E. Prati, "Waveguide dielectric permittivity measurement technique based on resonant FSS filters," *IEEE Microw. Wireless Compon. Lett.*, vol. 21, no. 5, pp. 273–275, May 2011.

[9] C.-K. Lee, S. Zhang, S. S. Bukhari, D. Cadman, J. Vardaxoglou, and W. G. Whittow, "Complex permittivity measurement system for solid materials using complementary frequency selective surfaces," *IEEE Access*, vol. 8, pp. 7628–7640, 2020.

[10] M.-S. Park, J. Cho, S. Lee, Y. Kwon, and K. Y. Jung, "New measurement technique for complex permittivity in millimeter-wave band using simple rectangular waveguide adapters," *J. Electromagn. Eng. Sci.*, vol. 22, no. 6, pp. 616–621, 2022.

[11] C.-S. Lee and C.-L. Yang, "Complementary split-ring resonators for measuring dielectric constants and loss tangents," *IEEE Microw. Wireless Compon. Lett.*, vol. 24, no. 8, pp. 563–565, Aug. 2014.

[12] A. M. Albishi, M. K. E. Badawe, V. Nayyeri, and O. M. Ramahi, "Enhancing the sensitivity of dielectric sensors with multiple coupled complementary split-ring resonators," *IEEE Trans. Microw. Theory Techn.*, vol. 68, no. 10, pp. 4340–4347, Oct. 2020.

[13] P. Vélez, L. Su, K. Grenier, J. Mata-Contreras, D. Dubuc, and F. Martín, "Microwave microfluidic sensor based on a microstrip splitter/combiner configuration and split ring resonators (SRRs) for dielectric characterization of liquids," *IEEE Sensors J.*, vol. 17, no. 20, pp. 6589–6598, Oct. 2017.

[14] S. Zahertar, E. Laurin, L. E. Dodd, and H. Torun, "Embroidered rectangular split-ring resonators for the characterization of dielectric materials," *IEEE Sensors J.*, vol. 20, no. 5, pp. 2434–2439, Mar. 2020.

[15] N. Pejman, S. Hashemi, A. Abdolali, M. Tayarani, and S. Moinzad, "Complex permittivity retrieval of dispersive liquids based on varactor-loaded split-ring resonator," *IEEE Sensors J.*, vol. 21, no. 21, pp. 24019–24027, Nov. 2021.

[16] A. Buragohain, A. T. T. Mostako, and G. S. Das, "Low-cost CSRR based sensor for determination of dielectric constant of liquid samples," *IEEE Sensors J.*, vol. 21, no. 24, pp. 27450–27457, Dec. 2021.

[17] S.-Y. Jang and J.-R. Yang, "Double split-ring resonator for dielectric constant measurement of solids and liquids," *J. Electromagn. Eng. Sci.*, vol. 22, no. 2, pp. 122–128, 2022.

[18] M. S. Boybay and O. M. Ramahi, "Material characterization using complementary split-ring resonators," *IEEE Trans. Instrum. Meas.*, vol. 61, no. 11, pp. 3039–3046, Nov. 2012.

[19] X.-C. Zhu, W. Hong, K. Wu, H.-J. Tang, Z.-C. Hao, and H.-X. Zhou, "Characterization of substrate material using complementary split ring resonators at terahertz frequencies," in *Proc. IEEE Int. Wireless Symp.*, 2013, pp. 1–4.

[20] M. Beruete, M. Sorolla, R. Marqués, J. Baena, and M. Freire, "Resonance and cross-polarization effects in conventional and complementary split ring resonator periodic screens," *Electromagnetics*, vol. 26, no. 3/4, pp. 247–260, 2006.

[21] W. Li, Y. Lan, H. Wang, and Y. Xu, "Microwave polarizer based on complementary split ring resonators frequency-selective surface for conformal application," *IEEE Access*, vol. 9, pp. 111383–111389, 2021.

[22] R. James, F. A. Fernandez, S. E. Day, S. Bulja, and D. Mirshekar-Syahkal, "Accurate modeling for wideband characterization of nematic liquid crystals for microwave applications," *IEEE Trans. Microw. Theory Techn.*, vol. 57, no. 12, pp. 3293–3297, Dec. 2009.

[23] D. Bourreau, A. Peden, and S. Le Maguer, "A quasi-optical free-space measurement setup without time-domain gating for material characterization in the *W*-band," *IEEE Trans. Instrum. Meas.*, vol. 55, no. 6, pp. 2022–2028, Dec. 2006.

[24] R. Dickie et al., "Electrical characterisation of liquid crystals at millimetre wavelengths using frequency selective surfaces," *Electron. Lett.*, vol. 48, no. 11, pp. 611–612, 2012.

[25] E. Polat et al., "Characterization of liquid crystals using a temperature-controlled 60 GHz resonator," in *Proc. IEEE MTT-S Int. Microw. Workshop Ser. Adv. Mater. Processes RF THz Appl.*, 2019, pp. 19–21.